ORIGINAL RESEARCH

Sustained cortical and subcortical neuromodulation induced by electrical tongue stimulation

**Joseph C. Wildenberg · Mitchell E. Tyler ·
Yuri P. Danilov · Kurt A. Kaczmarek ·
Mary E. Meyerand**

Abstract This pilot study aimed to show that information-free stimulation of the tongue can improve behavioral measures and induce sustained neuromodulation of the balance-processing network in individuals with balance dysfunction. Twelve balance-impaired subjects received one week of cranial nerve non-invasive neuromodulation (CN-NINM). Before and after the week of stimulation, postural sway and fMRI activation were measured to monitor susceptibility to optic flow. Nine normal controls also underwent the postural sway and fMRI tests but did not receive CN-NINM. Results showed that before CN-NINM balance-impaired subjects swayed more than normal controls as expected ($p \leq 0.05$), and that overall sway and susceptibility to optic flow decreased after CN-NINM ($p \leq 0.005$ & $p \leq 0.05$). fMRI showed upregulation of visual sensitivity to optic flow in balance-impaired subjects that decreased after CN-NINM. A region of interest analysis indicated that CN-NINM may induce neuromodulation by increasing activity within the dorsal pons ($p \leq 0.01$).

Keywords fMRI · Optic flow · Neuromodulation · Balance disorders · Brainstem · Plasticity

J. C. Wildenberg · M. E. Meyerand
Neuroscience Training Program,
University of Wisconsin-Madison,
Madison, WI 53705, USA

J. C. Wildenberg
Medical Scientist Training Program,
University of Wisconsin-Madison,
Madison, WI 53705, USA

M. E. Tyler · Y. P. Danilov · K. A. Kaczmarek
Department of Orthopedics and Rehabilitation,
University of Wisconsin-Madison,
Madison, WI 53705, USA

M. E. Meyerand
Department of Medical Physics,
University of Wisconsin-Madison,
Madison, WI 53705, USA

J. C. Wildenberg (✉)
1122o Wisconsin Institutes for Medical Research,
1111 Highland Ave.,
Madison, WI 53705, USA
e-mail: jcwildenberg@wisc.edu

Introduction

The idea of replacing information intended for one sensory modality with input to another was pioneered by Paul Bach-y-Rita during the late 1960's. Initially applied successfully to blind subjects through a tactile display (Kaczmarek and Bach-y-Rita 1995; Bach-y-Rita et al. 1969), sensory substitution is increasingly recognized as a simple yet effective therapy for many diseases that result in sensory impairment (Cesarani et al. 2004; Walker et al. 1997). Previously, our group and others have shown that the tongue can be used as an effective interface for sending signals to the central nervous system (Chebat et al. 2007; Bach-y-Rita and Kercel 2003; Sampaio et al. 2001; Bach-y-Rita et al. 1998). Compared to the skin, the tongue provides an inviting target for electrical neurostimulation due to the high electrolyte content of saliva, allowing for low-impedance electrical input, and the high density of sensory receptors permitting reasonably high throughput of incoming signals while preserving a relatively large dynamic

range (Lozano et al. 2009). Additionally, because tongue neurostimulation is non-invasive, it avoids a major drawback of other commonly-used types of electrical neurostimulation such as vagal nerve and deep brain stimulation while exhibiting less non-specific activation than other non-invasive modalities such as transcranial magnetic or direct current stimulation.

Our group has applied the concepts of sensory substitution to individuals with balance dysfunction by delivering head-position information measured with a head-mounted accelerometer via electrotactile neurostimulation of the tongue (Tyler et al. 2003). Previous studies using this technique have shown sensory substitution via electrical neurostimulation of the tongue to be effective at improving postural performance in both healthy and balance-impaired individuals (Robinson et al. 2009; Vuillerme and Cuisinier 2009; Vuillerme et al. 2008; Danilov et al. 2007; Danilov et al. 2006). The significance of these studies is both that electrical tongue stimulation aided these balance subjects in maintaining postural and gait stability, and also that some of the measured beneficial effects were sustained, lasting from days to weeks after stimulation sessions had ended. Additionally, these subjects had improved scores on standardized tests of balance and gait, and reported post-stimulation improvements in their subjective symptoms of dizziness, vertigo, and ability to concentrate. This therapy does not appear to be etiology specific, and beneficial effects are seen even in balance subjects who have exhausted all other treatment options, e.g. vestibular rehabilitation therapy. Cross-modal recruitment theories of plasticity can be used to explain why these subjects, as well as blind individuals trained to use the tongue's "tactile-visual acuity," show improvement in behavioral tasks using the stimulation for sensory substitution (Collignon et al. 2009; Pietrini et al. 2009; Poirier et al. 2007; Ptito et al. 2005). The remarkable retention effects on behavioral and subjective measures, extending long beyond the duration of the stimulation, do not entirely fit within this theoretical recruitment framework and must have some additional underlying mechanism.

Our current hypothesis to explain these sustained behavioral changes is based on neuroanatomy, observing that some cranial nerves have sensory afferents in the anterior tongue, i.e. the Lingual and Chorda Tympani branches of the Trigeminal (V) and Facial (VII) nerves, respectively. The brainstem projections of these nerves are the Trigeminal and Solitary nuclei, located immediately adjacent to the Vestibular nuclei near the dorsal aspect of the pontomedullary junction and extending superiorly through the pons (Fig. 1a). We postulate that stimulation of these cranial nerves may induce modulating activity in the Vestibular nuclei through interactions between these immediately adjacent structures, providing a mechanism by which stimulation of the tongue may influence balance processing.

We recently found that these sustained beneficial effects can be produced even when the stimulation signal carries no environmental information (sensory substitution is not a prerequisite to induce these effects). Preliminary data suggested that the electrotactile signal alone, devoid of any postural or gravitation information, is sufficient to improve neurorehabilitation in individuals with balance dysfunction. In line with our previous studies using sensory substitution, these subjects showed more rapid and greater recovery of function compared to those undergoing behavioral therapy (Danilov et al. 2007).

Based on the behavioral and subjective improvements seen in our previous studies, we believe electrical stimulation via the tongue can lead to network-wide neural changes that are sustained for multiple weeks beyond the last stimulation session. We have termed this process of information-free electrical tongue stimulation "cranial nerve non-invasive neuromodulation" or CN-NINM. In this proof-of-concept pilot study, we sought to confirm that the beneficial behavioral effects shown by previous sensory substitution studies were not due to the replacement of head-position information but were instead a product of the stimulation itself. Additionally, we utilized functional magnetic resonance imaging (fMRI) to detect the anatomical locations of any sustained neuromodulation induced by the electrical stimulation.

Methods

Subjects

Twelve subjects with chronic balance dysfunction (M/F: 6/6, mean age 52.2±10.3 years, Table 1) and nine normal controls (M/F: 5/4, mean age 50.4±12.8 years) participated in this study. Subjects completed consent, screening, and informational forms during their first visit. Since this was a pilot study, the inclusion criteria for the balance subjects were very broad. These criteria included anyone with a chronic, stable balance dysfunction that encompassed deficits of balance, posture, and gait. Exclusion criteria, for both balance subjects and controls, were pregnancy, mental health problems, corrected vision below 20/40, myasthenia gravis, Charcot-Marie Tooth disease, post-polio syndrome, Guillan-Barré, fibromyalgia, chronic fatigue syndrome, herniated disc and osteoarthritis of the spine. Exclusion criteria for balance subjects also included communicable diseases (HIV, TB, hepatitis, etc.), oral health problems (open sores in the mouth or tongue), and tongue neuropathies. Subjects were also excluded for the presence of MRI-incompatible metallic implants. The
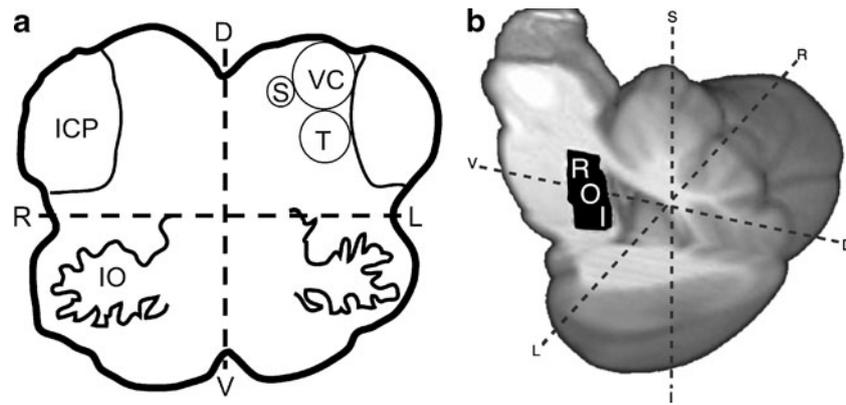
Fig. 1 Brainstem anatomy and ROI location. **a** Axial diagram of the brainstem at the pontomedullary junction shows the proximity of the Vestibular nuclei complex (VC) to the Trigeminal (T) and Solitary (S) nuclei, the apparent brainstem targets of CN-NINM. **b** A region of interest (ROI) was drawn on a high-resolution atlas of the brainstem and cerebellum (right) to analyze the BOLD signal changes in the area of overlap between the vestibular, trigeminal, and solitary nuclei bilaterally. *IO* Inferior Olive; *ICP* Inferior Cerebellar Peduncle; *L/R* Left/Right; *I/S* Inferior/Superior; *V/D* Ventral/Dorsal)

University of Wisconsin-Madison Health Sciences Institutional Review Board approved all aspects of this study and all subjects signed the approved consent form before beginning any portion of the study.

Visual stimuli and display

Two visual stimuli designed to induce postural sway and activate neural structures involved in balance processing were shown to subjects: static (CBstat) and 2-dimensional flow (CBrot) in which the image appears to cyclically approach and recede relative to the viewpoint as well as rotate about the center of the viewfield. A static checkerboard of alternating black and white squares was used for CBstat and as the basis for CBrot. CBstat had a square edge

length of 120 pixels and a total image size of 800×600 pixels (identical to the resolution of the display goggles). The dynamic stimulus was optimized to produce a strong sensation of egomotion through optic flow as this has been shown to increase postural responses (Kovacs et al. 2008; O'Connor et al. 2008; Slobounov et al. 2006; Kleinschmidt et al. 2002; Thurrell and Bronstein 2002). All motion was generated using sinusoids with the in/out motion following the equation

$$\text{square edge}_{\text{pixels}}(t) = 170 \sin(2\pi 0.2t + \Phi_{\text{io}}) + 230 \qquad (1)$$

The rotation was produced by the sum of two sinusoids using the equation

$$\theta_{\text{degrees}}(t) = 60(\sin(2\pi 0.2t + \Phi_{\text{rot1}}) + \sin(2\pi 0.35t + \Phi_{\text{rot2}})) \qquad (2)$$

(t is the time in seconds, θ is the global image rotation in degrees about the central point, Φ_{io} is the initial phase for the in/out motion, and Φ_{rot1} and Φ_{rot2} are the initial phases for the rotational motion). The superposition of two sinusoids was used for the rotational motion after preliminary results indicated that prediction of the rotation produced by a single sinusoid reduced the sensation of egomotion. Three versions of CBrot were produced with different initial phases to further reduce habituation and prediction of the motion. All versions of CBrot had a resolution of 800×600 pixels and were displayed at 60 frames-per-second.

Subjects viewed the visual stimuli on head-mounted display goggles (Resonance Technology, Northridge, CA). These goggles produce an 800×600 pixel display with a 30° horizontal and 22° vertical field-of-view in each eye. A mask of black fabric was placed over the subject's head and

Table 1 Age, sex, and clinical diagnosis of the twelve balance-impaired subjects enrolled in this study

Subject	Gender	Age	Clinical diagnosis
A	M	56	Central Vestibular Disorder
B	F	47	Migraine-related Balance Disorder
C	M	46	Traumatic Brain Injury
D	F	46	Chronic Ménière's Disease
E	M	38	Spinocerebellar Ataxia
F	F	66	Gentamicin Ototoxicity
G	M	64	Idiopathic Cerebellar Ataxia
H	F	43	Spinocerebellar Ataxia
I	M	44	Peripheral Vestibular Disorder
J	F	55	Peripheral Vestibular Disorder
K	F	51	Idiopathic Vestibular Disorder
J	M	73	Cerebellar Infarction

goggles to block all remaining ambient light. This goggle and mask setup were used for display of the visual stimuli in both the postural and fMRI tests.

Postural sway measurement

Subjects stood on the floor wearing a customized helmet fitted with a two-directional digital accelerometer to measure postural sway in response to the visual stimuli. Data from the helmet-mounted accelerometer was collected at 30 Hz using customized software.

MRI data collection

MRI data was acquired with the University of Wisconsin-Madison Department of Radiology's 3T clinical MRI scanner (GE Healthcare, Waukesha, WI). T1-weighted anatomical images were collected using a spoiled gradient recalled (3D-SPGR) pulse sequence. Functional scans were acquired with a T2*-weighted gradient-echo echo planar imaging sequence (TR=2,000 ms, echo time = 30 ms, flip angle = 75°) to acquire BOLD signal over a 64×64 matrix and 28 axial slices (3.75×3.75×5 mm resolution). Respiratory volume and cardiac waveforms were recorded at 40 Hz during functional scans for artifact reduction during data analysis. Balance subjects underwent two scans, one before and one after the stimulation regimen. Normal controls underwent one scan.

Tongue stimulation

Stimulation to the tongue was delivered via a small electrode array placed on the anterior portion of the tongue and held in place by pressure of the tongue to the roof of the mouth (Tyler et al. 2003). The array is a flexible polyester-base printed circuit containing 144 electrodes in a square matrix (Fig. 2a). The circular gold-plated electrodes are 1.55 mm in diameter with an on-center spacing of 2.32 mm. A custom-designed waveform generator delivered positive monophasic voltage pulses that were capacitively-coupled to the electrode array for zero net direct current. The maximal output voltage of the device was 24 V. The sensation produced by the array is similar to the feeling of drinking a carbonated beverage. To prevent possible disease transmission, the electrode array was sterilized using gluteraldehyde between subjects. Additionally, the array was cleaned with 91% isopropyl alcohol between every stimulation session.

CN-NINM stimulation consists of three square-pulse bursts with an intraburst frequency of 200 Hz and an interburst frequency of 50 Hz that does not vary throughout the duration of the stimulation session (Fig. 2b). This signal was delivered to all 144 electrodes of the array. Unlike our
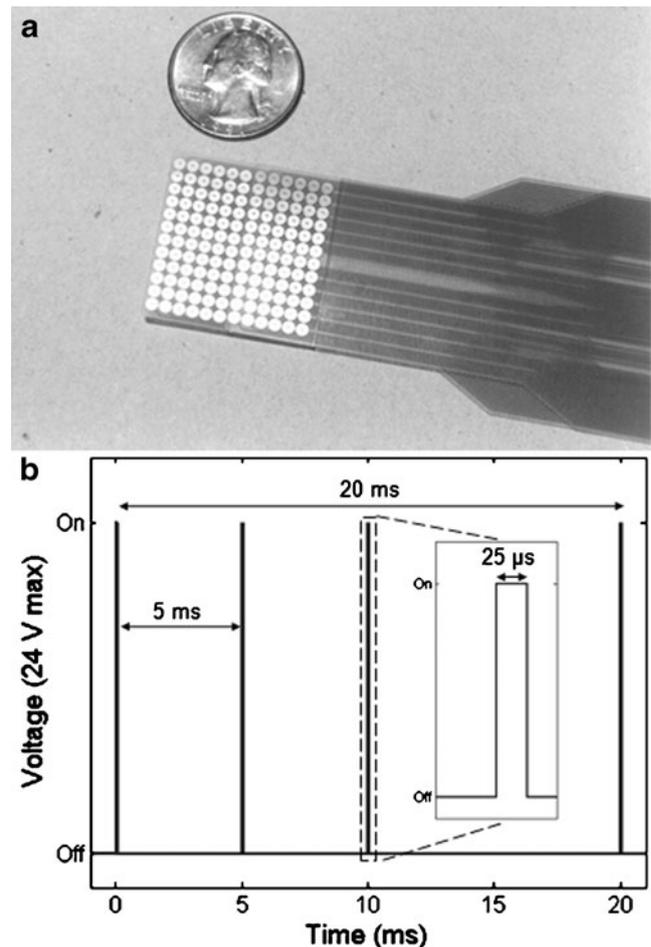

Fig. 2 Tongue stimulation device and CN-NINM waveform. **a** The 12×12 electrode array, here shown next to a quarter for reference, is placed on the anterior surface of the tongue and is held in place by pressure of the tongue to the roof of the mouth. **b** CN-NINM stimulation consists of three square-wave pulse bursts with a 200 Hz intraburst and 50 Hz interburst frequency. The stimulation voltage is adjusted at the start of every stimulation session and has a maximum of 24 V

previous studies, the electrical signal used did not vary with time or contain environmental cues and therefore did not provide any useful exogenous information to the subject (Danilov et al. 2006, 2007).

Procedure

On the day of the first visit (day 0, Pre-CN-NINM and Normal), all subjects were asked to stand with their feet together while wearing the display goggles and helmet-mounted accelerometer. To prevent falls, subjects wore a physical therapy harness throughout the duration of the experiment that allowed researchers to support the subject, if necessary, without restricting movement.

The postural sway experiment consisted of a 200-second run during which the visual stimuli were randomly

displayed in trials of 12 s alternated with 6 s of fixation to minimize contamination of sway due to the transition from one visual stimulus trial to the next (O'Connor et al. 2008). If a subject experienced a loss of balance, the trial number was noted for data analysis and the experiment continued after the subject regained their balance.

After completion of the postural sway experiment, subjects underwent an MRI scan to determine brain regions activated by the visual stimuli. Subjects wore the display goggles and mask, a respiratory belt, and a pulse oximeter while in the MRI scanner. During the functional scan, subjects were shown the visual stimuli using the same randomized block-design paradigm used for the postural sway experiment. However, the functional scan was 504 s in duration. No tongue stimulation was given during the postural sway or fMRI tests.

CN-NINM stimulation was delivered to the balance subjects over nine stimulation sessions (2 on days 1–4 and one on day 5). Before the start of the first stimulation session on day 1, subjects were familiarized with the electrode array and control box. At the start of every stimulation session subjects placed the electrode array on their tongue and adjusted the stimulation intensity to a comfortable level between the lower limit of sensation and a maximum level without discomfort. After approximately 1 min of continuous CN-NINM stimulation, during which the subject was instructed to manipulate the intensity to their preference, the level was set and subsequently maintained for that session.

After setting the CN-NINM stimulation level, subjects received continuous stimulation for 20 min, wherein the subject stood as still as possible with their eyes closed (one subject was unable to stand in this position without losing balance for the two stimulation sessions on day 1 and instead sat on a back-less stool. This subject was able to stand with eyes closed for the remainder of the stimulation sessions).

After the completion of the nine stimulation sessions, balance subjects repeated the postural sway and fMRI tests. The procedures for the tests on day 5 (Post-CN-NINM) were identical to those completed on day 0. Subjects performed these tests between three and six hours after the final stimulation session.

Postural sway data analysis

Data analysis for the postural sway tests was performed using MATLAB (The MathWorks, Inc.). Only data from the anterior-posterior sway was used for analysis as previous studies have shown increased sensitivity compared to left-right sway (Palmisano et al. 2009). Following procedures described by O'Connor et al. for analysis of head sway data, the anterior-posterior signal was filtered

with a 2nd order lowpass digital Butterworth filter with cutoff frequency of 2 Hz (O'Connor et al. 2008). The resulting signal was integrated to velocity and then squared to produce the instantaneous power of velocity. The average power of head sway velocity (P_{vel}) was computed separately for each of the 12-second trials. P_{vel} values from trials of like visual stimuli were averaged together, log-transformed, and expressed in dB ($10*\log(P_{vel})$, reference value of 1 degree^2/second^2) to stabilize the variance prior to statistical testing (Petrie and Sabin 2005).

Intergroup statistics were calculated from each subject's trial-averaged P_{vel} data (CBrot–CBstat contrast) using two-sample two-tailed t-tests. A two-way repeated measures ANOVA was conducted on the balance-subject's trial-averaged P_{vel} data expressed in dB using both the CBstat and CBrot P_{vel} values. The independent variables were task (*Task*: CBstat, CBrot) and time (*Time*: Pre-CN-NINM, Post-CN-NINM). Analyses included main effects and the two-way interaction using a significance cutoff of $p \leq 0.05$.

MRI data analysis

MRI data was preprocessed using AFNI (Cox 1996). This processing included corrections for slice-time acquisition errors, subject motion, and low-pass filtering of non-task-related noise (0.15 Hz cutoff). The general linear model (GLM) was estimated using SPM8. Percent signal change was calculated by dividing the difference in the estimated beta weights by the scan's baseline image. Physiologic data collected during the scanning sessions was processed using a script provided by Kelley et al. to extract useful information about respiratory and cardiac rhythms to include as regressors in the GLM (Kelley et al. 2008). Motion parameters, and these parameters shifted by one time-point, were also added as regressors to the GLM (Johnstone et al. 2006; Lund et al. 2005).

Two different post-GLM normalization techniques were used to align the cortex and subcortical structures separately. Cortical structures were normalized to the SPM8's ICBM152 atlas using the built-in normalization algorithm. All group cortical results are derived from data using this normalization procedure. Normalization of posterior fossa structures, for both the voxelwise and ROI analyses, were performed using the SUIT algorithm and atlas as this has been shown to more accurately align these small structures (Diedrichsen et al. 2009; Diedrichsen 2006). Both normalization techniques resampled the images to a resolution of $2\times2\times2$ mm using 7th-degree b-spline interpolation. Post-normalization smoothing of cortical images was performed with an isotropic Gaussian filter (8 mm FWHM) and subcortical structures with a 5 mm filter.

To focus on areas within the dorsal brainstem that contain the target sensory nuclei for CN-NINM a region of

interest (ROI) analysis was performed as the area is notoriously difficult to image due to low signal-to-noise and complications from cardiac and respiratory-related movement (Kovacs et al. 2006). This analysis allows the use of a priori anatomical and physiological information to lessen false-negatives introduced by corrections for multiple comparisons required in standard voxelwise techniques (Nichols and Hayasaka 2003). An *a priori* ROI with a volume of 3,040 μl was drawn on the SUIT atlas encompassing the dorsal pons using Duvernoy's brain stem atlas as a reference (Fig. 1b) (Duvernoy 1995). This ROI was defined by selecting the mid-point between ventral and dorsal edges of the central pons and including all neural tissue dorsal to that point bilaterally. The inferior border was defined by the inferior aspect of the inferior cerebellar peduncle and the superior border by the superior aspect of the superior cerebellar peduncle. The mean signal change of this ROI was extracted from each subject's scans normalized to the SUIT atlas.

Intergroup statistics for the fMRI data were calculated from the percent signal change (CBrot–CBstat contrast) using *t*-tests (one-sample for pre-CN-NINM, post-CN-NINM and normal control groups and two-sample for the post-norm and pre-norm comparisons). A two-way repeated measures ANOVA, identical to the one described for the postural sway analysis, was used to compare balance subjects pre-CN-NINM and post-CN-NINM. The displayed images and tables were created using paired *t*-tests to identify the directionality of the effect at each voxel. Corrections for multiple comparisons was performed using AFNI's *AlphaSim* Monte-Carlo simulations (Forman et al. 1995). This method allows for a combination of thresholding and spatial clustering to produce a corrected *p*-value. Results from these simulations indicated that only activation clusters thresholded at $\alpha \leq 0.001$ with a volume greater than 496 μl would have global significance at $p \leq 0.05$ for the cortical data smoothed with an 8 mm filter. The subcortical data filtered with a 5 mm filter required a volume greater than 128 μl using the same threshold. Only clusters with volumes greater than these cutoffs are displayed in the figures and tables.

Results

Postural sway results

Subject J was unable to complete the pre-CN-NINM postural sway tests due to nausea induced by travel to our facility and was therefore excluded from this analysis, but was able to complete the MRI scan and is included in that set of data. The effect of optic flow on postural sway was greater in balance subjects pre-CN-NINM than in controls

($p \leq 0.05$, Fig. 3). There was no difference in sway amplitude between balance subjects post-CN-NINM and controls. Balance subjects swayed more in response to the optic flow stimulus CBrot than the static stimulus CBstat (*Task*, $p \leq 0.005$). They also swayed more during the pre-CN-NINM tests than the post-CN-NINM tests (*Time*, $p \leq 0.005$). The magnitude of the optic flow effect appears to decrease after the CN-NINM stimulation (*Task × Time*, $p \leq 0.05$).

fMRI ROI results

Extracted signal changes within the dorsal pons ROI did not show any task or time dependence (Fig. 4). The magnitude of the effect of optic flow on the measured signal change in the ROI increased after stimulation (*Task× Time*, $p \leq 0.01$).

fMRI voxelwise results

Optic flow produced activation of the cuneus and lingual gyrus (V1), the lateral occipital gyrus (V5/MT), the superior parietal lobule (V3), and the posterior vermis of the cerebellum across all groups as analyzed by one-sample *t*-tests (Table 2, Fig. 4). The pre-CN-NINM group showed additional activations of the left cingulate sulcus visual area (CSv), the right superior marginal gyrus, the quadrangular lobe of the cerebellum, and deactivation of the right posterior insula (parieto-insular vestibular cortex; PIVC). The post-CN-NINM group showed activation of the right posterior thalamus and a region within the superior dorsal pons of the brainstem. Normal controls showed activation of the right CSv, the right posterior thalamus, and a bilateral area of the paracentral lobule. The cluster volumes from areas involved in visual motion processing were larger in
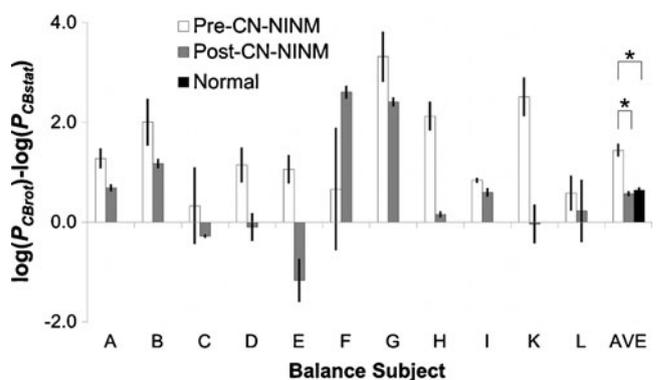

Fig. 3 Average difference of the power of head sway velocity (P_{vel}) measurements in response to the visual stimuli. The ANOVA showed a decreased sway in response to optic flow in the post-CN-NINM group compared to the pre-CN-NINM group. Two-sample *t*-tests show increased sway in the pre-CN-NINM group compared to the normal controls but no difference between the post-CN-NINM group and the controls. *Error bars* are the standard error of the mean. * - $p<0.05$
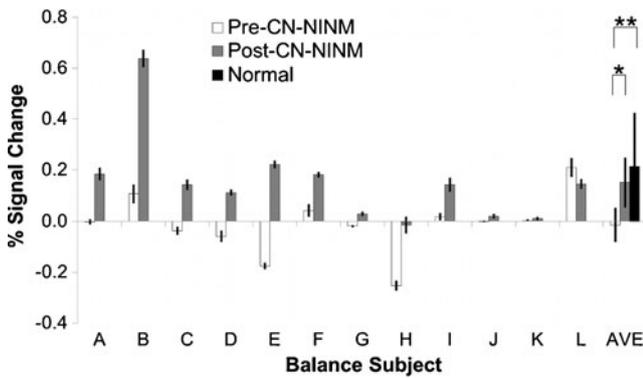
Fig. 4 The BOLD percent signal change of the CBrot–CBstat contrast for each subject averaged over the brainstem ROI. The ANOVA revealed increased activation in the post-CN-NINM group compared to the pre-CN-NINM group. Normal controls showed greater activation compared to the pre-CN-NINM group but not the post-CN-NINM group. *Error bars* are 95% confidence intervals about the mean. * - $p < 0.005$, ** - $p < 0.01$

the pre-CN-NINM group than normal controls. Intergroup comparisons using two-sample *t*-tests show more activation of the right superior marginal gyrus and V5/MT bilaterally in the pre-CN-NINM group than normal controls. There were no significant clusters of activation in the comparison of the post-CN-NINM group to the normal control group.

Comparison of the balance-impaired subjects before and after CN-NINM showed a similar task activation pattern to the one-sample *t*-tests above including V1, V3, V5/MT, the posterior vermis of the cerebellum, and deactivation of the PIVC (Table 3, Fig. 5). The superior marginal gyrus, medial frontal gyrus, and the quadrangular and biventer lobes of the cerebellum were also activated. There was time-dependent deactivations within the lingual gyrus bilaterally, and area of the lateral pons, and activation within the quadrangular lobe of the cerebellum. Two clusters of activation were significant for the interaction of time and task: a bilateral activation of the globus pallidus and a region in the right dorsal pons (Fig. 6).

Discussion

Consistent with previous studies evaluating the efficacy of electrical stimulation through the tongue coupled to head-position information, we found that simple electrical tongue stimulation, devoid of exogenous environmental information, can produce sustained beneficial behavioral effects. Optic flow produces compensatory sway and individuals with some balance dysfunction are hypersensitive, resulting

Table 2 Locations and volumes of significant clusters from the one- and two-sample *t*-tests of the CBrot–CBstat contrast. The center of mass for each cluster in x, y, and z coordinates is reported in MNI space

Region	R/L	Pre CN-NINM		Post CN-NINM		Normal		Pre-Norm	
		Coordinates	Vol. (μl)	Coordinates	Vol. (μl)	Coordinates	Vol. (μl)	Coordinates	Vol. (μl)
ICBM152 Atlas									
Cuneus	R	(20,83,25)	15,912	(22,82,26)	10,640	(26,79,22)	3,768		
	L	(−16,87,22)	4,888	(−14,87,24)	9,432	(−1,81,25)	9,272		
SPL	R			(20,63,66)	1,112				
	L			(−27,59,62)	1,072				
Lingual Gyrus	B	(2,75,−1)	4,992			(1,70,−3)	3,504		
	R			(32,73,−14)	1,312				
	L			(−13,73,−14)	3,024	(−20,90,−18)	608		
LOG	R	(48,67,1)	9,392	(48,72,−1)	4,704	(43,75,−8)	1,528	(40,78,9)	1,264
	L	(−43,74,0)	5,056	(−45,75,−1)	1,888	(−45,74,4)	3,136	(−39,73,2)	496
P. Insula	R	(45,19,8)#	2,256						
P. Cingulate	L	(−13,22,42)	1,344			(−14,22,48)	584		
SMG	R	(58,39,24)	864					(27,77,35)	3,904
Thalamus	R			(19,23,−1)	704	(25,30,5)	552		
Paracentral L.	B					(3,65,64)	640		
SUIT Atlas									
A. Vermis	B	(0, −71, −33)	144	(4, 64, −38)	328	(1, 71, −41)	216		
Quadrangular	R	(15, 70, −18)	152						
D. Pons	B			(0, −36, −23)	200				

SPL superior parietal lobule; *LOG* lateral occipital gyrus; *SMG* superior marginal gyrus; *L* lobule; *A/P* anterior/posterior; *R/L/B* right/left/bilateral, *D* dorsal; # decreased activation

Table 3 Locations and volumes of significant clusters from the ANOVA comparing the pre-CN-NINM to post-CN-NINM groups. The center of mass for each cluster in x, y, and z coordinates is reported in MNI space

Region	R/L	Task		Time		Task × Time	
		Coordinates	Vol. (µl)	Coordinates	Vol. (µl)	Coordinates	Vol. (µl)
ICBM152 Atlas							
Cuneus	R	(19,82,30)	10,744				
	L	(−16,84,29)	5,232				
SPL	R	(19,54,66)	7,704				
	L	(−24,58,61)	5,008				
Lingual Gyrus	R			(13,54,5)	2,240		
	L			(−12,43,5)	496		
	B	(2,73,3)	14,744				
LOG	R	(49,68,−1)	12,984				
	L	(−44,73,−1)	8,560				
P. Insula	R	(48,15,1)#	560				
P. Cingulate	R	(15,20,47)	2,208				
	L	(−14,21,44)	2,520				
SMG	R	(61,36,21)	4,496				
	R	(34,40,55)	784				
	L	(−32,45,56)	1,136				
MFG	R	(48,1,55)	696				
GP	B					(−2,−5,−3)	856
SUIT Atlas							
P. Vermis	B	(0,69,−35)	1,096				
Quadrangular	R	(11,72,−20)	280				
	L	(−13,73,−17)	184	(−13,67,−26)	152		
Biventer Lobule	R	(23,51,−47)	240				
D. Pons	L			(−5,32,−20)#	200		
	B					(3,38,−25)	128
M. Pons	R			(13,35,−39)#	176		

SPL superior parietal lobule; *LOG* lateral occipital gyrus; *SMG* superior marginal gyrus; *MFG* medial frontal gyrus; *GP* globus pallidus; *A/P* anterior/posterior; *R/L/B* right/left/bilateral, *D* dorsal; *M* medial; # decreased activation

in an exaggerated response (Mergner et al. 2005; Redfern and Furman 1994; van Asten et al. 1988). We saw reductions both in overall sway and sway in response to optic flow after the week of CN-NINM intervention. Additionally, we saw a significant difference between the balance-impaired subjects and normal controls before CN-NINM that was not present after CN-NINM. While we did not control for the repeated exposure to optic flow in the balance-impaired subjects, it is unlikely that sustained adaptation/habituation to optic flow could explain the behavioral improvements as we are exposed to equivalent visual stimuli during everyday life.

The functional imaging results indicate that the behavioral improvements due to CN-NINM are likely related to modulation of neural activity within structures of the balance-processing network. In particular, the ROI analysis showed an increase in BOLD signal within the dorsal pons

in response to optic flow after CN-NINM as compared to each subject's baseline. The significant area of activation in the dorsal pons found in the time x task interaction from the voxelwise ANOVA analysis is contained within the ROI and supports the a priori choice of the anatomical location. This same brainstem activation pattern was observed in healthy individuals by Bense and colleagues using horizontal optokinetic stimulation (Bense et al. 2006), and could be anticipated by the functional and anatomical connections between the structures putatively involved in balance processing and control.

The activation patterns across all groups are consistent with several previous studies investigating optic flow in both normal controls and balance-impaired individuals. These areas include multiple regions within the visual cortices, the CSv, the PIVC, and the posterior vermis of the cerebellum (Kikuchi et al. 2009; Ohlendorf et al. 2008;
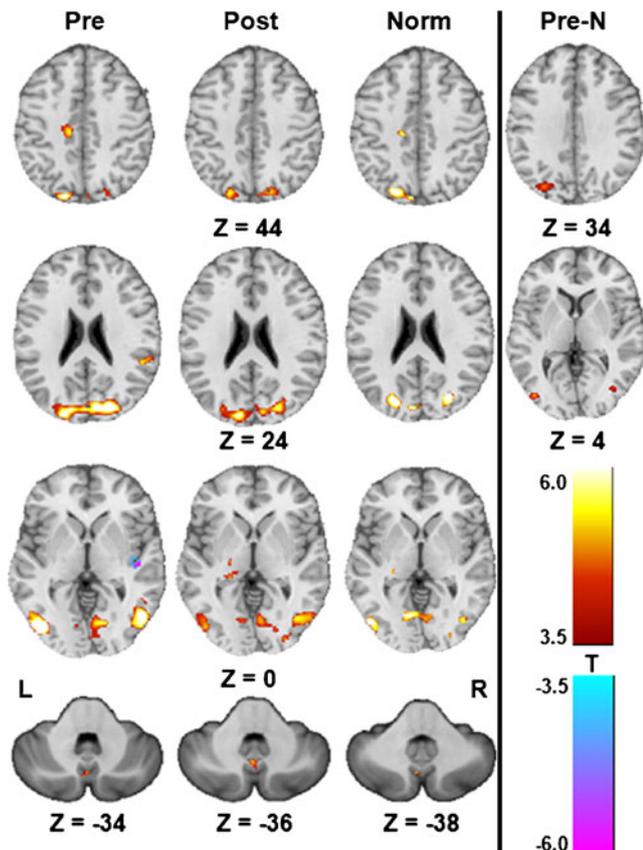
Fig. 5 Activation patterns of the CBrot–CBstat contrast from the one-sample *t*-tests (Pre: pre-CN-NINM, Post: post-CN-NINM, Norm: normal controls) and the two-sample *t*-test comparing the pre-CN-NINM group to normal controls (Pre-N). All images are thresholded at $\alpha \leq 0.001$ ($|T_{11}| \geq 4.0$ for Pre and Post, $|T_8| \geq 4.5$ for Norm, and $|T_{20}| \geq 3.5$ for Pre-N). Only clusters with a volume greater than 496 μl (128 μl for subcortical structures) are displayed. All Z values are in MNI coordinates

Slobounov et al. 2006; Dieterich et al. 2003; Dieterich and Brandt 2000; Sunaert et al. 1999; Cardin and Smith 2010). The increased activation seen in the balance subjects pre-CN-NINM compared to controls, as measured both by *t*-test comparison and cluster volume differences, supports the hypothesis by Dieterich and colleagues that balance dysfunction leads to upregulation and increased sensitivity of the visual system to motion in the visual field (Dieterich et al. 2007). This hypersensitivity of the visual system may be related to the exaggerated postural responses to optic flow of balance-impaired individuals compared to normal controls (Mergner et al. 2005; Redfern and Furman 1994). It is possible that this upregulation is no longer necessary after CN-NINM, which seems to rebalance activity within the network during optic flow processing. This could explain the activation patterns of balance subjects after CN-NINM, which appear similar to those of normal controls. This re-balancing of network activity would also be consistent with the abovementioned decrease in the

magnitude of the effect of optic flow on postural sway after CN-NINM.

The nuclei of the basal ganglia have been shown in previous studies to be activated during perceived self-motion and during vestibular stimulation accompanied by visual stimulation (Kovacs et al. 2008; Indovina et al. 2005; Deutschlander et al. 2004; Previc et al. 2000). While we have not yet developed a hypothesis for why the globus pallidus is more active in subjects after CN-NINM, it is possible the effects within the brainstem may be propagating to higher cortical and subcortial structures; thereby indirectly driving their responses to optical flow stimuli toward patterns similar to those of an unaffected individual.

These results support studies showing the capacity of neurostimulation to potentiate cross-modal plasticity in blind subjects and improvements in recovery and neural reorganization in stroke patients (Bolognini et al. 2009; Williams et al. 2009; Boggio et al. 2007; Celnik et al. 2007; Kupers et al. 2006; Webster et al. 2006; Ptito et al. 2005). However, unlike the stimulation procedures used in those studies, subjects in this study did not receive any explicit behavioral training and were not exposed to specific stimuli (e.g. optic flow) associated with the stimulation.

The sustained neuromodulatory effect we measured is in contrast with the theories and observations of other types of electrical neurostimulation (deep brain stimulation, vagal nerve stimulation, cochlear implants, etc.) in which the behavioral effects disappear when the stimulator is turned off/removed (Hammond et al. 2008). Recently, Canals et al. showed a similar lasting effect in rats using electrodes implanted in the hippocampus (Canals et al. 2009). Their study provides a mechanistic proof-of-concept for how local electrical induction of long-term potentiation (LTP) at the level of the individual neuron can result in global changes in activity within neural networks. Our study extends these findings by showing that changes in network dynamics induced by electrical neurostimulation can be seen without directly driving the network but instead during normal network processing i.e. our stimulation procedure does not include a visual component yet the network is processing visual stimuli differently after CN-NINM. Additionally, as was seen in the Canals study, we observed selective recruitment of cortical and subcortical structures that are a subset of the anatomically described network. For example, we did not see modulation of activity within the flocculus of the cerebellum, even though there are known bi-directional projections between it and the vestibular nuclei of the brainstem (Langer et al. 1985). This suggests CN-NINM does not uniformly affect the network but may be dependent on pre-existing connectivity and/or concurrent activation of the network by other means.

In addition to the behavioral deficits seen in subjects with balance disorders, it is likely that the dizziness and vertigo

experienced by balance-impaired individuals are due, in part, to abnormal processing of sensory inputs (Borel et al. 2008; Dieterich 2007). Loss of the sensory structures, such as in subjects with aminoglycoside-induced ototoxicity, may result in improper signal integration by the balance-processing centers. Subjects who have undergone therapy with electrical tongue stimulation report improvements in symptoms thought to be unrelated to the anatomical targets of the stimulation (Danilov et al. 2007). These improvements and the network-wide fMRI changes presented here further support the hypothesis that sustained neuromodulation extends beyond locally targeted regions. Based on the observed postural and fMRI results, we believe stimulation with CN-NINM induces wide-ranging neuroplastic changes allowing the brain to be more capable of properly integrating diverse sensory input. We also believe changes in cortical activity most likely arise through changes in processing and subsequent improvement in the quality of information sent from subcortical structures, through the thalamus, to the cortex (modulation of functional connectivity). This is consistent with a PET study indicating that the stimulation signal propagates through the thalamus to multiple cortical regions (Ptito et al. 2005). We have confirmed that both local and network-wide effects of electrical neurostimulation can persist after the stimulator is removed, consistent with previous behavioral studies using a similar technique (Danilov et al. 2006, 2007). We did not investigate the sustained effects of CN-NINM during other behavioral tasks nor did we measure neural activity elicited directly by the stimulation. It is therefore possible that the stimulation has much more diffuse effects than those presented here.

At the cellular level these sustained changes may be due to modulation of activity within the vestibular nuclei due to the stimulation arriving via the trigeminal nerves. Multiple studies, using electrical stimulation, electrophysiology, and neuronal tracers, in both humans and animal models, have established reciprocal projections between the sensory trigeminal and vestibular nuclei (Satoh et al. 2009; Marano et al. 2005; Anker et al. 2003; Herrick and Keifer 2000; Buisseret-Delmas et al. 1999). These projections provide a route by which stimulation of the tongue can modulate the balance processing network. The sustained effects are likely due to alterations in synaptic efficiency (re-weighting of inputs) and/or recruitment of other brain regions into the processing network. It is also possible for electrical stimulation to activate neural stem cells, many of which line the fourth ventricle adjacent to the dorsal pons (Yamada et al. 2007; Charrier et al. 2006). Additionally, the effects could be produced by modulation of natural neural oscillatory circuits, similar to theories of how deep brain stimulation (DBS), another information-free form of neurostimulation, produces behavioral changes in patients with Parkinson's disease (Fuentes et al. 2009; Montgomery and Gale 2008).

This study was limited by the absence of data collected from balance-impaired subjects using a placebo stimulation paradigm. The intense visitation requirements for this week-long study impeded our ability to recruit balance-impaired subjects willing to be randomly assigned to a placebo group. Additionally, the tactile sensation of tongue stimulation, noticeable even at low stimulation intensities, would reveal to subjects their treatment assignment. Finally, a randomized-control trial limited to peripheral vestibular dysfunction patients using very similar techniques is currently underway. Despite the lack of a control group, we believe the postural sway and fMRI changes measured
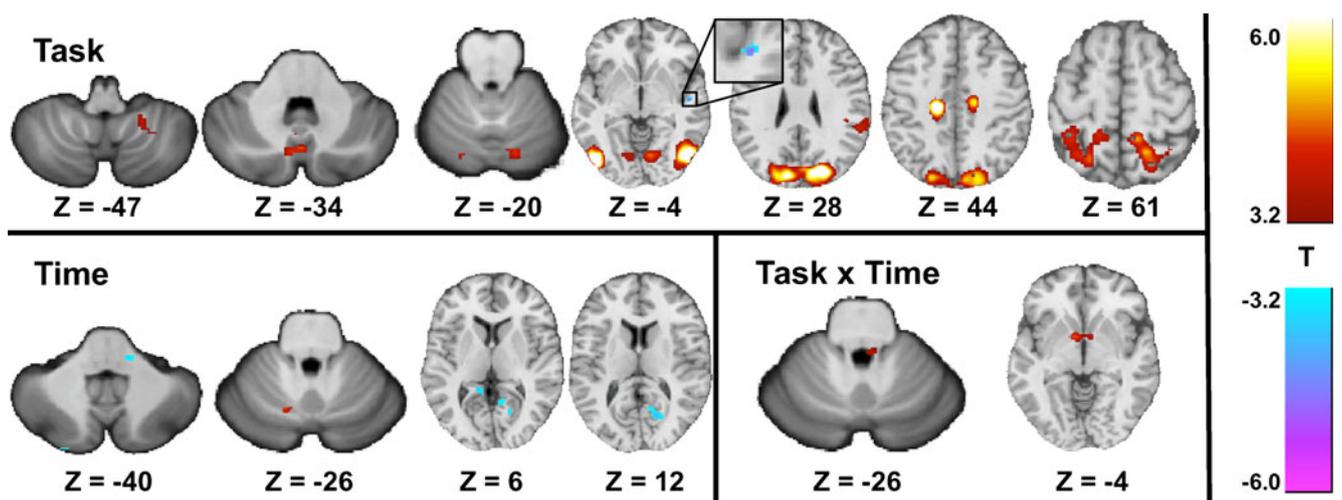

Fig. 6 Activation patterns from the ANOVA analysis comparing the pre-CN-NINM group to the post-CN-NINM group. Images are thresholded at $\alpha \leq 0.001$ ($|T_{44}| \geq 3.2$). Only clusters with a volume greater than 496 µl (128 µl for subcortical structures) are displayed. All Z values are in MNI coordinates

in this study are the result of CN-NINM stimulation. The inclusion of only chronic balance-impaired subjects makes spontaneous recovery unlikely and the mild balance tasks performed by the subjects are less intense than standard physical therapy—a treatment all of the balance subjects in this study had already rejected as being ineffective. Future work will investigate both the placebo response as well as how the stimulation effects healthy controls.

This study included a heterogeneous balance-impaired subject population. Although these subjects had different etiologies as diagnosed by their physician, they are united by deficits of balance, gait, and posture. The effect of optic flow on postural stability measured in this study are consistent both with previous studies including only peripheral vestibular patients and those with a heterogeneous balance-impaired population (Mergner et al. 2005; Redfern and Furman 1994). While imaging studies have shown differential activation patterns between central and peripheral vestibular patients using direct galvanic or caloric stimulation, these differences are expected as the anatomical structures used as input also contain the lesions (Dieterich and Brandt 2008). Optic flow, conversely, uses the visual system to activate the balance-processing centers. The activation patterns of the heterogeneous population included in this study are very similar to those from an fMRI study investigating the response of peripheral vestibular patients to optic flow (Dieterich et al. 2007).

The ability to non-invasively stimulate targeted regions of the central nervous system to produce lasting beneficial effects opens up the possibility for at-home therapies for neurological disorders that can be utilized as needed without constant medical supervision. The results also point to the opportunity to increase the rate and extent of neurorehabilitation by making interventions available more frequently (i.e. twice daily as was demonstrated in this study, versus a single weekly or biweekly outsubject visit). Finally, the recent rapid increase in the number of medical conditions treated by invasive neurostimulation has expanded the need for non-invasive, effective alternatives (Miller 2009).

References

Anker, A. R., Ali, A., Arendt, H. E., Cass, S. P., Cotter, L. A., Jian, B. J., et al. (2003). Use of electrical vestibular stimulation to alter genioglossal muscle activity in awake cats. *Journal of Vestibular Research, 13*, 1–8.

Bach-y-Rita, P., Collins, C. C., Saunders, F. A., White, B., & Scadden, L. (1969). Vision substitution by tactile image projection. *Nature, 221*, 963–964.

Bach-y-Rita, P., Kaczmarek, K. A., Tyler, M. E., & Garcia-Lara, J. (1998). Form perception with a 49-point electrotactile stimulus array on the tongue: a technical note. *Journal of Rehabilitation Research and Development, 35*, 427–430.

Bach-y-Rita, P., & Kercel, S. W. (2003). Sensory substitution and the human–machine interface. *Trends in Cognitive Sciences, 7*, 541–546.

Bense, S., Janusch, B., Vucurevic, G., Bauermann, T., Schlindwein, P., Brandt, T., et al. (2006). Brainstem and cerebellar fMRI-activation during horizontal and vertical optokinetic stimulation. *Experimental Brain Research, 174*, 312–323.

Boggio, P. S., Nunes, A., Rigonatti, S. P., Nitsche, M. A., Pascual-Leone, A., & Fregni, F. (2007). Repeated sessions of noninvasive brain DC stimulation is associated with motor function improvement in stroke patients. *Restorative Neurology and Neuroscience, 25*, 123–129.

Bolognini, N., Pascual-Leone, A., & Fregni, F. (2009). Using non-invasive brain stimulation to augment motor training-induced plasticity. *Journal of Neuroengineering and Rehabilitation, 6*, 6–8.

Borel, L., Lopez, C., Péruch, P., & Lacour, M. (2008). Vestibular syndrome: a change in internal spatial representation. *Neurophysiologie Clinique/Clinical Neurophysiology, 38*, 375–389.

Buisseret-Delmas, C., Compoint, C., Delfini, C., & Buisseret, P. (1999). Organisation of reciprocal connections between trigeminal and vestibular nuclei in the rat. *Journal of Comparative Neurology, 409*, 153–168.

Canals, S., Beyerlein, M., Merkle, H., & Logothetis, N. K. (2009). Functional MRI evidence for LTP-induced neural network reorganization. *Current Biology, 19*, 398–403.

Cardin, V., & Smith, A. T. (2010). Sensitivity of human visual and vestibular cortical regions to egomotion-compatible visual stimulation. *Cerebral Cortex*, doi:10.1093/cercor/bhp268.

Celnik, P., Hummel, F., Harris-Love, M., Wolk, R., & Cohen, L. G. (2007). Somatosensory stimulation enhances the effects of training functional hand tasks in patients with chronic stroke. *Archives of Physical Medicine and Rehabilitation, 88*, 1369–1376.

Cesarani, A., Alpini, D., Monti, B., & Raponi, G. (2004). The treatment of acute vertigo. *Neurological Sciences, 25*, 26–30.

Charrier, C., Coronas, V., Fombonne, J., Roger, M., Jean, A., Krantic, S., et al. (2006). Characterization of neural stem cells in the dorsal vagal complex of adult rat by in vivo proliferation labeling and in vitro neurosphere assay. *Neuroscience, 138*, 5–16.

Chebat, D. R., Rainville, C., Kupers, R., & Ptito, M. (2007). Tactile-'visual'acuity of the tongue in early blind individuals. *Neuroreport, 18*, 1901–1904.

Collignon, O., Voss, P., Lassonde, M., & Lepore, F. (2009). Cross-modal plasticity for the spatial processing of sounds in visually deprived subjects. *Experimental Brain Research, 192*, 343–358.

Cox, R. W. (1996). AFNI: software for analysis and visualization of functional magnetic resonance neuroimages. *Computers and Biomedical Research, 29*, 162–173.

Danilov, Y. P., Tyler, M. E., Skinner, K. L., & Bach-y-Rita, P. (2006). Efficacy of electrotactile vestibular substitution in patients with bilateral vestibular and central balance loss. *Conference Proceedings—IEEE Engineering in Medicine and Biology Society, Suppl,* 6605–6609.

Danilov, Y., Tyler, M., Skinner, K., Hogle, R., & Bach-y-Rita, P. (2007). Efficacy of electrotactile vestibular substitution in patients with peripheral and central vestibular loss. *Journal of Vestibular Research, 17*, 119–130.

Deutschlander, A., Bense, S., Stephan, T., Schwaiger, M., Dieterich, M., & Brandt, T. (2004). Rollvection versus linearvection: comparison of brain activations in PET. *Human Brain Mapping, 21*, 143–153.

Diedrichsen, J. (2006). A spatially unbiased atlas template of the human cerebellum. *Neuroimage, 33*, 127–138.

Diedrichsen, J., Balsters, J. H., Flavell, J., Cussans, E., & Ramnani, N. (2009). A probabilistic MR atlas of the human cerebellum. *Neuroimage, 46*, 39–46.

Dieterich, M. (2007). Central vestibular disorders. *Journal of Neurology, 254*, 559–568.

Dieterich, M., & Brandt, T. (2000). Brain activation studies on visual-vestibular and ocular motor interaction. *Current Opinion in Neurology, 13*, 13.

Dieterich, M., & Brandt, T. (2008). Functional brain imaging of peripheral and central vestibular disorders. *Brain, 131*, 2538–2552.

Dieterich, M., Bense, S., Stephan, T., Yousry, T. A., & Brandt, T. (2003). fMRI signal increases and decreases in cortical areas during small-field optokinetic stimulation and central fixation. *Experimental Brain Research, 148*, 117–127.

Dieterich, M., Bauermann, T., Best, C., Stoeter, P., & Schlindwein, P. (2007). Evidence for cortical visual substitution of chronic bilateral vestibular failure (an fMRI study). *Brain, 130*, 2108–2116.

Duvernoy, H. M. (1995). *The human brain stem and cerebellum* (p. 430). New York: Springer-Verlag.

Forman, S. D., Cohen, J. D., Fitzgerald, M., Eddy, W. F., Mintun, M. A., & Noll, D. C. (1995). Improved assessment of significant activation in functional magnetic resonance imaging (fMRI): use of a cluster-size threshold. *Magnetic Resonance in Medicine, 33*, 636–647.

Fuentes, R., Petersson, P., Siesser, W. B., Caron, M. G., & Nicolelis, M. A. L. (2009). Spinal cord stimulation restores locomotion in animal models of Parkinson's disease. *Science, 323*, 1578.

Hammond, C., Ammari, R., Bioulac, B., & Garcia, L. (2008). Latest view on the mechanism of action of deep brain stimulation. *Movement Disorders, 23*, 2111–2121.

Herrick, J. L., & Keifer, J. (2000). Central Trigeminal and Posterior Eighth Nerve Projections in the Turtle *Chrysemys picta* Studied in vitro. *Brain, Behavior and Evolution, 51*, 183–201.

Indovina, I., Maffei, V., Bosco, G., Zago, M., Macaluso, E., & Lacquaniti, F. (2005). Representation of visual gravitational motion in the human vestibular cortex. *Science, 308*, 416–419.

Johnstone, T., Ores Walsh, K. S., Greischar, L. L., Alexander, A. L., Fox, A. S., Davidson, R. J., et al. (2006). Motion correction and the use of motion covariates in multiple-subject fMRI analysis. *Human Brain Mapping, 27*, 779–788.

Kaczmarek, K. A., & Bach-y-Rita, P. (1995). Tactile displays. In W. Barfield & T. A. Furness (Eds.), *Virtual environments and advanced interface design* (pp. 349–414). USA: Oxford University Press.

Kelley, D. J., Oakes, T. R., Greischar, L. L., Chung, M. K., Ollinger, J. M., & Greene, E. (2008). Automatic physiological waveform processing for fMRI noise correction and analysis. *PLoS ONE, 3*, e1751.

Kikuchi, M., Naito, Y., Senda, M., Okada, T., Shinohara, S., Fujiwara, K., et al. (2009). Cortical activation during optokinetic stimulation—an fMRI study. *Acta Oto-laryngologica, 129*, 440–443.

Kleinschmidt, A., Thilo, K. V., Buchel, C., Gresty, M. A., Bronstein, A. M., & Frackowiak, R. S. J. (2002). Neural correlates of visual-motion perception as object-or self-motion. *Neuroimage, 16*, 873–882.

Kovacs, S., Peeters, R., Smits, M., De Ridder, D., Van Hecke, P., & Sunaert, S. (2006). Activation of cortical and subcortical auditory structures at 3T by means of a functional magnetic resonance imaging paradigm suitable for clinical use. *Investigative Radiology, 41*, 87–96.

Kovacs, G., Raabe, M., & Greenlee, M. W. (2008). Neural correlates of visually induced self-motion illusion in depth. *Cerebral Cortex, 18*, 1779–1787.

Kupers, R., Fumal, A., de Noordhout, A. M., Gjedde, A., Schoenen, J., & Ptito, M. (2006). Transcranial magnetic stimulation of the visual cortex induces somatotopically organized qualia in blind subjects. *Proceedings of the National Academy of Sciences, 103*, 13256–13260.

Langer, T., Fuchs, A. F., Scudder, C. A., & Chubb, M. C. (1985). Afferents to the flocculus of the cerebellum in the rhesus macaque as revealed by retrograde transport of horseradish peroxidase. *Journal of Comparative Neurology, 235*, 1–25.

Lozano, C. A., Kaczmarek, K. A., & Santello, M. (2009). Electrotactile stimulation on the tongue: intensity perception, discrimination, and cross-modality estimation. *Somatosensory & Motor Research, 26*, 50–63.

Lund, T. E., Nørgaard, M. D., Rostrup, E., Rowe, J. B., & Paulson, O. B. (2005). Motion or activity: their role in intra-and inter-subject variation in fMRI. *Neuroimage, 26*, 960–964.

Marano, E., Marcelli, V., Stasio, E. D., Bonuso, S., Vacca, G., Manganelli, F., et al. (2005). Trigeminal stimulation elicits a peripheral vestibular imbalance in migraine patients. *Headache: the Journal of Head and Face Pain, 45*, 325–331.

Mergner, T., Schweigart, G., Maurer, C., & Blümle, A. (2005). Human postural responses to motion of real and virtual visual environments under different support base conditions. *Experimental Brain Research, 167*, 535–556.

Miller, G. (2009). Neuropsychiatry. Rewiring faulty circuits in the brain. *Science, 323*, 1554–1556.

Montgomery, E. B., & Gale, J. T. (2008). Mechanisms of action of deep brain stimulation (DBS). *Neuroscience and Biobehavioral Reviews, 32*, 388–407.

Nichols, T., & Hayasaka, S. (2003). Controlling the familywise error rate in functional neuroimaging: a comparative review. *Statistical Methods in Medical Research, 12*, 419–446.

O'Connor, K. W., Loughlin, P. J., Redfern, M. S., & Sparto, P. J. (2008). Postural adaptations to repeated optic flow stimulation in older adults. *Gait & Posture, 28*, 385–391.

Ohlendorf, S., Sprenger, A., Speck, O., Haller, S., & Kimmig, H. (2008). Optic flow stimuli in and near the visual field centre: a group fMRI study of motion sensitive regions. *PLoS ONE, 3*, e4043.

Palmisano, S., Pinniger, G. J., Ash, A., & Steele, J. R. (2009). Effects of simulated viewpoint jitter on visually induced postural sway. *Perception, 38*, 442–453.

Petrie, A., & Sabin, C. (2005). *Medical statistics at a glance*. Malden: Wiley-Blackwell. 160 pp.

Pietrini, P., Ptito, M., & Kupers, R. (2009). Blindness and consciousness: New light from the dark. In S. Laureys, & G. Tononi G (Eds.), *The neurology of consciousness*. New York: Academic Press, pp. 360–374.

Poirier, C., De Volder, A. G., & Scheiber, C. (2007). What neuroimaging tells us about sensory substitution. *Neuroscience and Biobehavioral Reviews, 31*, 1064–1070.

Previc, F. H., Liotti, M., Blakemore, C., Beer, J., & Fox, P. (2000). Functional imaging of brain areas involved in the processing of

coherent and incoherent wide field-of-view visual motion. *Experimental Brain Research, 131*, 393–405.

Ptito, M., Moesgaard, S. M., Gjedde, A., & Kupers, R. (2005). Cross-modal plasticity revealed by electrotactile stimulation of the tongue in the congenitally blind. *Brain, 128*, 606.

Redfern, M. S., & Furman, J. M. (1994). Postural sway of patients with vestibular disorders during optic flow. *Journal of Vestibular Research, 4*, 221–230.

Robinson, B. S., Cook, J. L., Richburg, C. M. C., & Price, S. E. (2009). Use of an electrotactile vestibular substitution system to facilitate balance and gait of an individual with gentamicin-induced bilateral vestibular hypofunction and bilateral transtibial amputation. *Journal of Neurologic Physical Therapy, 33*, 150–159.

Sampaio, E., Maris, S., & Bach-y-Rita, P. (2001). Brain plasticity:'-visual'acuity of blind persons via the tongue. *Brain Research, 908*, 204–207.

Satoh, Y., Ishizuka, K. I., & Murakami, T. (2009). Modulation of the masseteric monosynaptic reflex by stimulation of the vestibular nuclear complex in rats. *Neurosci Lett, 466*, 16–20.

Slobounov, S., Wu, T., Hallett, M., Shibasaki, H., Slobounov, E., & Newell, K. (2006). Neural underpinning of postural responses to visual field motion. *Biological Psychology, 72*, 188–197.

Sunaert, S., Van Hecke, P., Marchal, G., & Orban, G. A. (1999). Motion-responsive regions of the human brain. *Experimental Brain Research, 127*, 355–370.

Thurrell, A., & Bronstein, A. (2002). Vection increases the magnitude and accuracy of visually evoked postural responses. *Experimental Brain Research, 147*, 558–560.

Tyler, M., Danilov, Y., & Bach-Y-Rita, P. (2003). Closing an open-loop control system: vestibular substitution through the tongue. *Journal of Integrative Neuroscience, 2*, 159–164.

van Asten, W., Gielen, C., & Gon, J. J. D. (1988). Postural adjustments induced by simulated motion of differently structured environments. *Experimental Brain Research, 73*, 371–383.

Vuillerme, N., & Cuisinier, R. (2009). Sensory supplementation through tongue electrotactile stimulation to preserve head stabilization in space in the absence of vision. *Investigative Ophthalmology & Visual Science, 50*, 476–481.

Vuillerme, N., Pinsault, N., Fleury, A., Chenu, O., Demongeot, J., Payan, Y., et al. (2008). Effectiveness of an electro-tactile vestibular substitution system in improving upright postural control in unilateral vestibular-defective patients. *Gait Posture, 28*, 711–715.

Walker, S. C., Helm, P. A., & Lavery, L. A. (1997). Gait pattern alteration by functional sensory substitution in healthy subjects and in diabetic subjects with peripheral neuropathy. *Archives of Physical Medicine and Rehabilitation, 78*, 853–856.

Webster, B. R., Celnik, P. A., & Cohen, L. G. (2006). Noninvasive brain stimulation in stroke rehabilitation. *NeuroRx, 3*, 474–481.

Williams, J. A., Imamura, M., & Fregni, F. (2009). Updates on the use of non-invasive brain stimulation in physical and rehabilitation medicine. *Journal of Rehabilitation Medicine, 41*, 305–311.

Yamada, M., Tanemura, K., Okada, S., Iwanami, A., Nakamura, M., Mizuno, H., et al. (2007). Electrical stimulation modulates fate determination of differentiating embryonic stem cells. *Stem Cells, 25*, 562–570.